




SHORT COMMUNICATION

Spontaneous xenogeneic GvHD in Wilms' tumor Patient-Derived xenograft models and potential solutions

Seyed Mostafa Monzavi^{1,2,3}  | Ahad Muhammadnejad^{4,5} | Maryam Behfar⁶ | Amir Arsalan Khorsand^{3,5} | Samad Muhammadnejad^{3,5,6}  | Abdol-Mohammad Kajbafzadeh^{1,2,5} 

¹Department of Applied Cell Sciences, School of Advanced Technologies in Medicine, Tehran University of Medical Sciences, Tehran, Iran

²Pediatric Urology and Regenerative Medicine Research Center, Tehran University of Medical Sciences, Tehran, Iran

³Gene Therapy Research Center, Digestive Diseases Research Institute, Tehran University of Medical Sciences, Tehran, Iran

⁴Cancer Biology Research Center, Cancer Institute of Iran, Tehran University of Medical Sciences, Tehran, Iran

⁵PDX Platform, Biomarker Evaluation and Supervision Team for Personalized Medicine, Molecular Tumor Board, Cancer Institute of Iran, Tehran University of Medical Sciences, Tehran, Iran

⁶Pediatric Cell and Gene Therapy Research Center, Tehran University of Medical Sciences, Tehran, Iran

Correspondence

Samad Muhammadnejad, Gene Therapy Research Center, Digestive Diseases Research Institute, Shariati Hospital, Tehran University of Medical Sciences (TUMS), Tehran, Iran.
Email: smuhammadnejad@gmail.com

Abdol-Mohammad Kajbafzadeh, Pediatric Urology and Regenerative Medicine, Children's Medical Center, Tehran University of Medical Sciences, Tehran, Iran.
Email: kajbafzd@tums.ac.ir

Funding information

Tehran University of Medical Sciences and Health Services, Grant/Award Number: TUMS-38292

Abstract

Severely immunocompromised NOD.Cg-Prkdc^{scid}Il2rg^{tm1Sug} (NOG) mice are among the ideal animal recipients for generation of human cancer models. Transplantation of human solid tumors having abundant tumor-infiltrating lymphocytes (TILs) can induce xenogeneic graft-versus-host disease (xGvHD) following engraftment and expansion of the TILs inside the animal body. Wilms' tumor (WT) has not been recognized as a lymphocyte-predominant tumor. However, 3 consecutive generations of NOG mice bearing WT patient-derived xenografts (PDX) xenotransplanted from a single donor showed different degrees of inflammatory symptoms after transplantation before any therapeutic intervention. In the initial generation, dermatitis, auto-amputation of digits, weight loss, lymphadenopathy, hepatitis, and interstitial pneumonitis were observed. Despite antibiotic treatment, no response was noticed, and thus the animals were prematurely euthanized (day 47 posttransplantation). Laboratory and histopathologic evaluations revealed lymphoid infiltrates positively immunostained with anti-human CD3 and CD8 antibodies in the xenografts and primary tumor, whereas no microbial infection or lymphoproliferative disorder was found. Mice of the next generation that lived longer (91 days) developed sclerotic skin changes and more severe pneumonitis. Cutaneous symptoms were milder in the last generation. The xenografts of the last 2 generations also contained TILs, and lacked lymphoproliferative transformation. The systemic immunoinflammatory syndrome in the absence of

Seyed Mostafa Monzavi and Ahad Muhammadnejad contributed equally to this work.

This is an open access article under the terms of the [Creative Commons Attribution-NonCommercial-NoDerivs](https://creativecommons.org/licenses/by-nc-nd/4.0/) License, which permits use and distribution in any medium, provided the original work is properly cited, the use is non-commercial and no modifications or adaptations are made.

© 2022 The Authors. *Animal Models and Experimental Medicine* published by John Wiley & Sons Australia, Ltd on behalf of The Chinese Association for Laboratory Animal Sciences.

microbial infection and posttransplant lymphoproliferative disorder was suggestive of xGvHD. While there are few reports of xGvHD in severely immunodeficient mice xenotransplanted from lymphodominant tumor xenografts, this report for the first time documented serial xGvHD in consecutive passages of WT PDX-bearing models and discussed potential solutions to prevent such an undesired complication.

KEYWORDS

graft-versus-host disease, patient-derived xenograft models, tumor-infiltrating lymphocytes, Wilms' tumor

1 | INTRODUCTION

Severely immunocompromised non-obese diabetic (NOD) mice bearing mutations for *Prkdc*, the severe combined immunodeficiency (SCID) mutation, and interleukin-2R γ (*IL-2R γ*) genes, also known as NOD.Cg-*Prkdc*^{scid} *Il2rg*^{tm1Sug} (NOG) strain, are among the ideal animal recipients for generation of cancer models.^{1,2} In adoptive immunotherapy research or xenotransplantation of lymphodominant grafts, these mice are vulnerable to develop xenogeneic graft-versus-host disease (xGvHD) following engraftment of transplanted or cotransplanted immune cells with xenogeneic origin, especially if the animal was not formerly humanized.² Wilms' tumor (WT), known as the most common primary renal tumor in childhood, has not generally been recognized as a lymphocyte-predominant solid tumor.³ However, a series of NOG mice in our lab acquired an immunoinflammatory syndrome after transplantation of a patient-derived WT xenograft before any therapeutic intervention, which later was confirmed to be xGvHD owing to engraftment and expansion of the primary graft-originated tumor-infiltrating lymphocytes (TILs) in the animal body. This is especially important for PDX platforms offering services for personalized medicine or preclinical drug-development research to consider some pre-xenotransplantation precautions. Regarding this, some potential solutions to prevent such an undesired event have also been reviewed in this paper.

2 | METHODS

A series of 8-10-week male NOG mice, used for generation of WT patient-derived xenograft (PDX) models, expressed inflammatory cutaneous signs shortly after tumor implantation in consecutive passages (Figure 1A). The primary tumor specimen (parental tumor) was collected from a 10-month-old infant who underwent radical nephrectomy with the diagnosis of histologically unfavorable WT. The tumor specimen had a bloody appearance and was immediately transferred to tissue processing lab and washed in a biosafety cabinet using sterile DMEM supplemented with 1x penicillin/streptomycin and amphotericin B, and fractionated (3-4 mm³ tumor fragments). The bloody appearance of the tumor tissue modestly decreased after the washing step. Subsequently, the tumor fragments

were transferred to animal facility. The colony of mice was kept in a temperature-controlled clean room with HEPA-filtered air (PDX Core Laboratory of Digestive Diseases Research Institute, TUMS, Iran), housed in separate positive pressure individually ventilated cages (Tecniplast S.p.A., Buguggiate, Italy) containing aspen chip bedding (2-3 mice per cage). Four to 5 fragments per animal were implanted subcutaneously into 2 NOG mice at right flank to produce the F₀ generation of the PDX models. The mice were receiving sterile commercial diet and acidified water ad libitum. The colony was free of minute virus of mice, mouse encephalomyelitis virus, mouse hepatitis virus, mouse parvovirus, pneumonia virus of mice, mouse rotavirus, murine norovirus, ectromelia virus, Hantaan virus, K virus, reovirus 3, lymphocytic choriomeningitis virus, mouse adenovirus types 1 and 2 (FL and K87), polyoma virus, mouse cytomegalovirus, Sendai virus, mouse thymic virus, lactate dehydrogenase elevating virus; β -hemolytic *Streptococcus*, *Mycoplasma pulmonis*, *Citrobacter rodentium*, *Corynebacterium bovis*, *Salmonella* spp., *Staphylococcus aureus*, *Enterococcus* spp., *Proteus* spp., *Clostridium piliforme*; and fur parasites (*Myobia musculi*, *Myocoptes musculinis*, *Psorergates simplex*, *Radfordia affinis*, *Polyplax spinulosa*), *Syphacia* spp., *Spironucleus muris*, *Aspicularis tetraptera*, *Giardia muris*, *Ornithonyssus bacoti*, and *Encephalitozoon cuniculi*. Body condition (BC) of the mice was assessed according to the scoring system developed by Ullman-Culleré and Foltz.⁴

After euthanasia, the formalin-fixed paraffin-embedded tissue specimens were used and processed for hematoxylin and eosin (HE) and immunohistochemical (IHC) staining for specific surface markers (i.e., human CD3, 4, and 8, and programmed death-ligand 1 [PDL1]). The immunostained pathology slides for CD markers were observed and evaluated using Allred scoring system, which considers 2 features:⁵ (1) the estimated proportion of positively stained cells; which is scored on the basis of a 5-tier scale (i.e., "0" for none, "1" for <1%, "2" for 1-10%, "3" for 11-33%, "4" for 34-66%, and "5" for >66% of total cells are stained cells); (2) the average intensity of staining in the positively stained cells, which is scored on the basis of a 3-tier scale (i.e., "1" for weak, "2" for intermediate, and "3" for strong intensity). The sum of the 2 scores represents the total Allred score (ranging from 0 to 8), and ≤ 2 is generally interpreted as negative. The extent of PDL1 expression was reported on the basis of tumor proportion score $(\frac{\text{Number of PDL1-positive tumor cells}}{\text{Total number of viable tumor cells}} \times 100)$.⁶

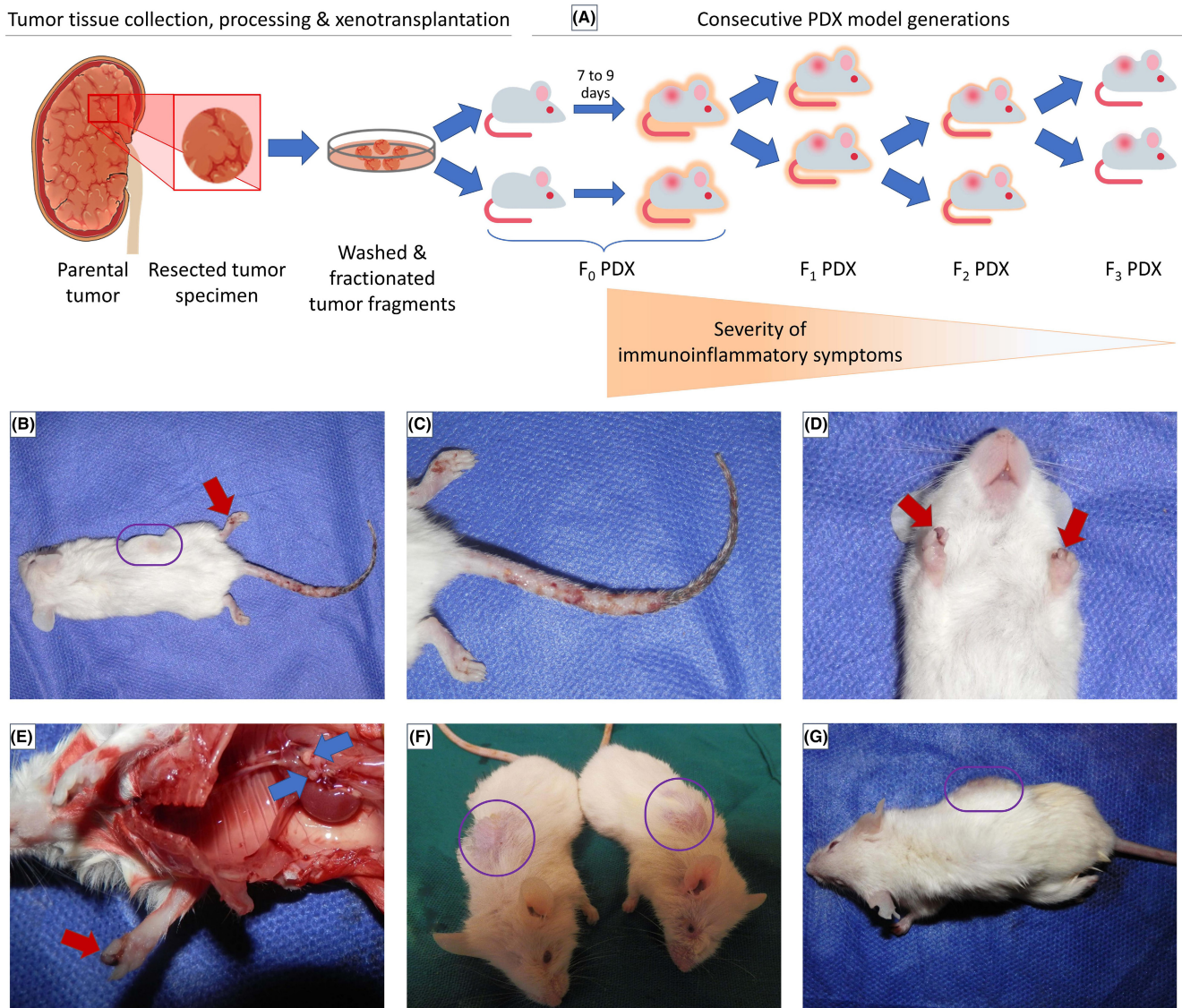


FIGURE 1 Outline of the PDX development and images of consecutive generations of PDX models. (A) the process of PDX development and graphical presentation of the extent of immunoinflammatory syndrome in different generations of the PDX models. (B) F₀ PDX model with tumor formation, scruffy hair coat, and severe inflammatory cutaneous signs on the tail and digits (day 47 posttransplantation). (C) Tail of the F₀ PDX model with extensive desquamation and crusting ulcers (day 47). (D) Perioral alopecia and autoamputation of the forepaws in the F₀ PDX model (day 47). (E) Lumbo-aortic lymphadenopathy in the F₀ PDX model (day 47). (F) F₁ PDX models with weight loss, scruffy hair coat, and conjunctival erythema (day 91). (G) F₂ PDX model with scruffy hair coat and limited desquamation of the tail (day 89).

3 | RESULTS

3.1 | Initial generation

One week after tumor implantation, we observed conjunctival erythema and mild scruffy hair coat in the F₀ WT PDX mice. As soon as noticing these manifestations, enrofloxacin was added to the drinking water (1.9 ml of 22.7 mg/mL to a 250ml bottle for 10 days) of the 2 WT PDX-bearing mice, while no response to this treatment was witnessed. After 4 weeks, nail loss of forepaws, scaling of the tail skin, moderate scruffy hair coat, and dermatitis developed concurrently with considerable tumor growth in the flank. Until the end of the 6th week, the mice had normal body condition (BC3). In the 7th

week, when the tumor size exceeded 500mm,³ relative emaciation (BC2), total desquamation of the tail, auto-amputation of digits of fore and hindlimbs, and hindlimb paresis occurred in the mice, which resulted in impaired locomotor activity (Figure 1B-E). To ethically prevent the unnecessary suffering from the illness, the mice were euthanized (day 47 posttransplantation). It is noteworthy that the mice of other projects in other cages in the colony did not show any similar signs. After necropsy, adenopathy of lumbo-aortic (Inn. Lumbales aortici) lymph nodes (Figure 1E) and pulmonary hyperemia were found; however, no other gross pathology on other organs was evident.

Possible differential diagnoses for the cutaneous manifestations included: microbial infections (e.g., mouse adenovirus,

Corynebacterium bovis, *Enterococcus* spp., and fungal and parasite infestation) and fighting trauma. Tests for the mentioned potential microbial infections turned out to be negative. Hence, given the simultaneous presence of conjunctival erythema, dermatitis, pulmonary inflammation, and lymphadenopathy, a type of systemic immunoinflammatory disorder was suggested. Microscopic studies of HE-stained tissue slides of the euthanized F_0 animals revealed (Figure 2)¹: scattered lymphocyte infiltration in the tumor specimen,² extravasation of lymphocytes and perivascular lymphocytic infiltration in the skin,³ interstitial pneumonitis with remodeling phenomenon and diffuse lymphocyte infiltration in the lung,⁴ focal adenitis with giant-cell-like lymphocytes in the lymph nodes, and⁵ lymphocytic infiltration between hepatocytes in the liver. To confirm the observation of lymphocytes within the tumor specimen, immunostaining for CD3 marker was performed and revealed positive cells in the blastemal and epithelial components. This necessitated histological examination of the paraffin-embedded parental tumor, where diffuse infiltration of CD3⁺ and CD8⁺ cells in blastemal and epithelial components, and CD4⁺ cells in mesenchymal component, was found (Figure 2, Table 1). In addition, the lung specimens of F_0 mice were found to contain CD3⁺ cells, which is confirmatory evidence of human-originated lymphocytes. The presence of the lymphoid infiltrates in different organs of the animals inherently lacking functional lymphocytes and natural killer cells, and the presence of TILs within the parental and F_0 tumor were the key clues, and considering the mentioned set of clinical signs, were suggestive of xGvHD in the PDX mice. Lymphadenopathy could also suggest Epstein-Barr virus (EBV) infection of cotransplanted TILs in the primary graft. Nonetheless, the absence of lymphoproliferative transformation in the F_0 HE-stained tumor slides ruled out such diagnosis (Figure 2).

3.2 | Subsequent generations

After passaging the F_0 tumor xenograft to the next generation (2 mice), that is, the mice bearing the first filial generation (F_1) of the PDX; scruffy hair coat started to appear in the 3rd week. The mice were at BC3 until the end of 12th week, but then they started to emaciate (BC2). Moreover, their skin mildly thickened and lost flexibility, when gradually scattered alopecia emerged, suggesting a pre-scleroderma state. However, nail loss, extensive desquamation of the tail, and auto-amputation of digits did not occur in this generation (Figure 1F). The tumor size grew exponentially to over 2000 mm³ (a commonly accepted ethical cutoff for euthanasia) until the middle of the 13th week (day 91). Thus, the mice were euthanized; in necropsy, lymphadenopathy was absent, but pulmonary congestion was observed. HE-stained lung slides were compatible with pneumonitis and emphysematous changes along with abundant lymphocyte infiltrates. In HE-stained skin slides, lymphocyte infiltrations in dermis, increased density of connective tissue, and chronic keratinization were evident. HE-stained liver slides showed intrahepatocyte areas infiltrated with lymphocytes. The IHC slides of the F_1 tumor tissues were positive for CD3 and 8, but not for CD4.

In the subsequent generation of the PDX models, that is, F_2 mice, some of the clinical signs observed in the F_1 mice repeated, but were less severe (Figure 1G). Mild scruffy hair coat occurred, but with no histologic evidence of cutaneous inflammation and no lymphoid infiltrates. In the pathology slides of other tissues of F_2 mice, liver was involved with lymphoid infiltrates and no pulmonary inflammation or lymphoid infiltrate was detected, while, again, the tumor contained CD3- and CD8-positive cells (Figure 2). It is noteworthy that the F_2 mice were euthanized at day 89 when they were still at BC3 and their tumor grew to over 2000 mm³. In general, more organs became involved in the F_0 mice than F_1 and F_2 mice, though the severity of pulmonary manifestations in F_1 mice was greater than in the 2 other generations. It should be noted that the F_0 mice were euthanized prematurely with a suspicion of pathogen contamination, and the F_1 mice lived longer (compared with the F_0 mice). Thus, the TILs had sufficient time to affect the mouse tissues, and consequently, development of chronic skin changes and severer pulmonary symptoms in the F_1 generation can be justified.

Lymphoproliferative lesions were not detected in the HE-stained slides of the F_1 and F_2 tumors, which further confirmed the ruling out of the potential diagnosis of EBV infection of TILs. Evaluated according to the Allred score, the CD3, CD4, and CD8 positivity in the tumor tissues decreased from parental (primary) tumor to the F_0 and then through to the F_2 mice. PDL1 positivity was 2% and over 5% in the parental tumor and the F_2 generation, respectively. Flowcytometry revealed 6.5%–7.2% human-origin CD3⁺ cells in the peripheral blood of the F_2 mice (Supporting Information). In the F_3 generation, the syndrome subsided considerably with none of the above-mentioned manifestations, but no pathologic or flowcytometric assays were performed, because a drug response assay was planned to be carried out in a precision medicine setting, and thus, this can be considered as a limitation to this report. It is of note that no peripheral blood of F_0 and F_1 generations was collected to undergo flow cytometry, and this may be seen as another limitation of this report. However, since the human-originated CD3⁺ cells were present in the peripheral blood of F_2 mice, it can be postulated that the CD3⁺ cells were also present in the 2 previous generations.

4 | DISCUSSION

With a successful background in generating WT PDX-bearing nude mice,⁷ we have recently started establishment of a national biorepository of WT PDX-bearing NOG mice. In this report, we described a series of spontaneous immunoinflammatory syndrome in severely immunocompromised mice transplanted with serial passages of a WT PDX. In the absence of evidence of microbial infection or lymphoproliferative transformation, and given the histopathologic and flowcytometric findings, xGvHD was the most probable cause. The underlying mechanism of this inflammatory response can be explained on the basis of the following potential events¹: WT patient-derived xenografts were engrafted successfully in the mice and subsequently became interlayered with murine stroma and

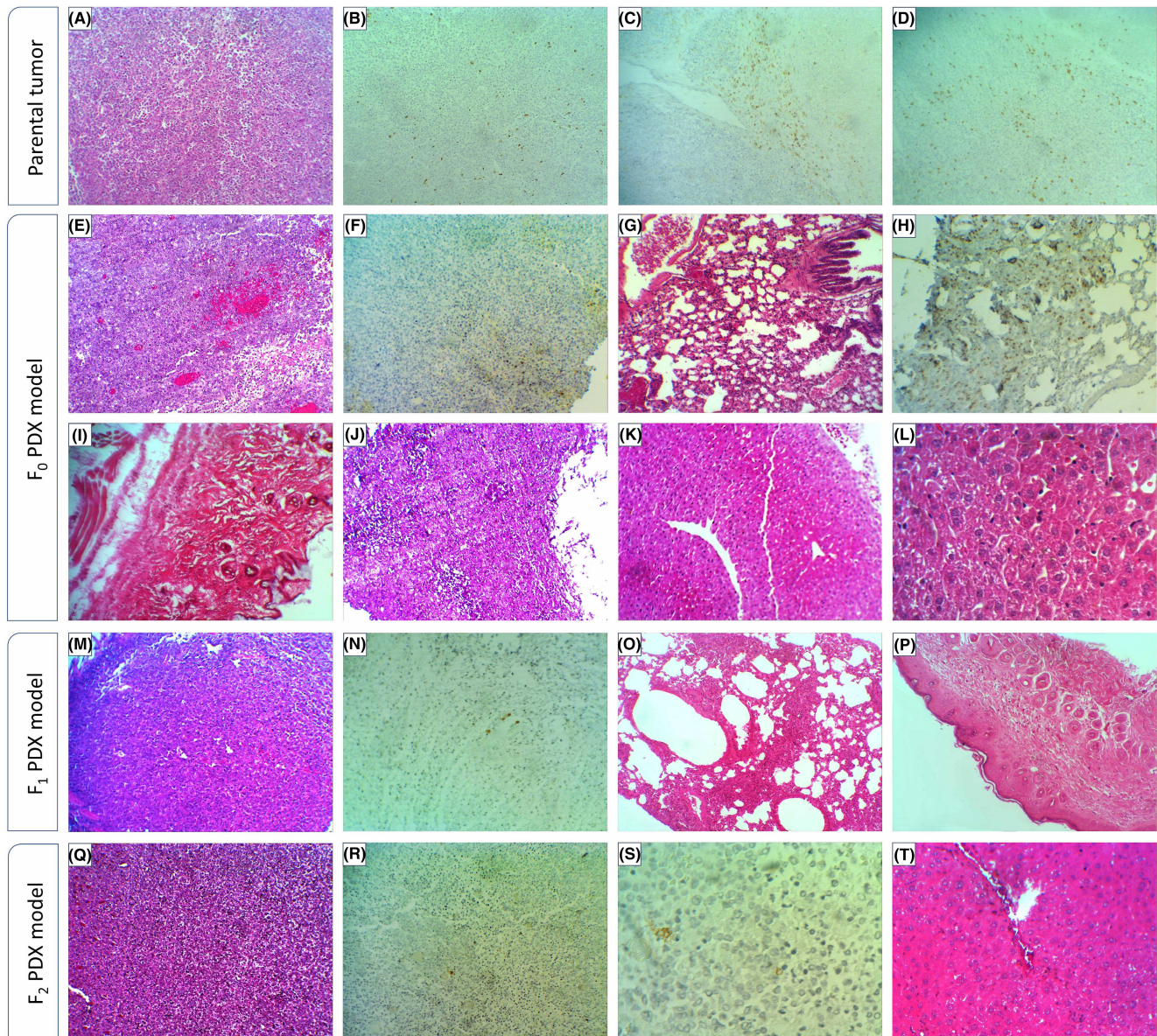


FIGURE 2 Pathological evaluation of the parental tumor and PDX models tissues. (A) Parental tumor composed of 65% epithelial, 25% blastemal, and 10% mesenchymal components (H&E, $\times 100$). (B) Parental tumor with several CD3⁺ cells (CD3 IHC, $\times 100$). (C) Parental tumor with several CD4⁺ cells (CD4 IHC, $\times 100$). (D) Parental tumor with several CD8⁺ cells (CD8 IHC, $\times 100$). (E) F₀ PDX tumor composed of 60% epithelial, 30% blastemal, and 10% mesenchymal components + blood vessels (H&E, $\times 100$). (F) F₀ PDX tumor with several CD3⁺ cells (CD3 IHC, $\times 100$). (G) Interstitial pneumonitis, with lymphocyte infiltration in alveolar and peribronchial regions in the lung of F₀ PDX model (H&E, $\times 100$). (H) Multiple CD3⁺ cells in interstitial tissue of the lung of F₀ PDX model (CD3 IHC, $\times 100$). (I) Relatively normal dermis and epidermis, limited number of lymphocytes between dermis and hypodermis (H&E, $\times 100$). (J) Multifocal adenitis with giant-cell-like lymphocytes within the lymph node of the F₁ PDX model. (K, L) Diffuse infiltration of lymphocytes in intrasinusoidal region and portal area with hemosiderin deposition in the liver of the F₀ PDX model (H&E, $\times 100$ and $\times 400$). (M) F₁ PDX tumor composed of 50% epithelial, 40% blastemal, and 10% mesenchymal components (H&E, $\times 100$). (N) F₁ PDX tumor with a number of CD3⁺ cells (CD3 IHC, $\times 100$). (O) Interstitial pneumonitis, emphysematous changes with lymphocyte infiltration in the alveolar and peribronchial regions in the lung of F₁ PDX model (H&E, $\times 100$). (P) Keratinization, sclerotic changes, and lymphocyte infiltration in dermis, causing increased density of connective tissue (H&E, $\times 100$). (Q) F₂ PDX tumor composed of 30% epithelial, 60% blastemal, and 10% mesenchymal components (H&E, $\times 100$). (R) F₂ PDX tumor with a few CD3⁺ cells (CD3 IHC, $\times 100$). (S) F₂ PDX tumor with a few CD8⁺ cells (CD8 IHC, $\times 400$). (T) Normal architecture with lymphocyte infiltration between hepatocytes in the liver of F₂ PDX model (H&E, $\times 400$).

supported with murine microvasculature²; high number of TILs inside the primary tumor (primary xenograft) gained an opportunity to traffic across the murine vascular endothelium and circulate in the blood throughout the animal body³; the (human-originated)

lymphocytes freely expanded inside the mouse hematologic system devoid of immune system confrontation functioned as a good incubator for the xenogeneic immune cells⁴; the human lymphocytes mismatching MHC system of the NOG mice invaded the normal

TABLE 1 Pathological evaluation of TILs in the parental tumor tissue and subsequent tumor xenografts

Generation	No. of TILs in H&E slides ^a	Immunohistochemical staining					
		CD3		CD4		CD8	
		No. of stained cells ^a	Allred score	No. of stained cells ^a	Allred score	No. of stained cells ^a	Allred score
Parental	15	17	5	8	4	14	5
F0, mouse#1	10	9	5	0	0	7	5
F0, mouse#2	8	7	4	0	0	6	4
F1, mouse#1	5	5	3	0	0	4	3
F1, mouse#2	4	4	3	0	0	4	3
F2, mouse#1	3	2	3	0	0	3	3
F2, mouse#2	1	2	3	0	0	1	3

^aCell counts are presented per 10 high-power fields of the tumor tissue.

tissues of the mice, causing an inflammatory syndrome with classic manifestations of GvHD.

The generation of PDX models of different malignancies, for use in preclinical drug testing, in vivo biology studies, biomarker profiling, and personalized medicine, has increasingly prospered in recent years.^{8,9} For successful implantation of the tumor tissue and bypassing the intrinsic immune system of the animal, severely immunodeficient mice, including NOG and NSG mice, are the animal of choice. These mice have the advantage of enhanced engraftment of heterologous cells.^{1,10} However, lack of a protecting immune system has made them vulnerable to invasion by xenogeneic immune cells, thereby causing xGvHD or lymphoproliferative disorder.^{11,12}

Generation of xGvHD models is desirable for scientists with a research focus on the GvHD itself.¹³ However, development of spontaneous xGvHD in solid tumor PDX models is a major confounder but underreported complication.^{11,14,15} Bondarenko et al. found metastatic T-cell lesions in PDX models xenotransplanted from solid tumor specimens (breast, colorectal, pancreatic, bladder, and renal cancer).¹⁴ Tilman et al. reported posttransplant lymphoproliferations in different organs of one-third of their PDX-bearing NSG mice that were xenotransplanted with hepatoblastoma, rhabdomyosarcoma, and osteosarcoma xenografts from pediatric donors.¹⁶ Likewise, Radaelli et al. reported immunoinflammatory syndrome in 12% of NOG mice xenografted with patient-derived metastatic melanomas. They attributed the manifestations to cotransplanted TILs within the melanoma tumor graft.¹⁵ The occurrence of such an unwanted event (xGvHD) in "melanoma PDX models" is quite expectable given that the melanoma is classified among the highly immunogenic tumors with high TIL density,¹⁷ and a proper candidate for immune checkpoint inhibitor treatments.^{18,19} However, for WT, which is not listed among lymphocyte-predominant solid tumors,^{3,20} the incidence of xGvHD in PDX models has been unexpected and not been reported elsewhere. Not only in xenografting of the solid tumors, but also in hematologic malignancies, the presence of cotransplanted lymphocytes can¹ mask the engraftment of the original

tumor,² develop posttransplant lymphoproliferative disorder, or³ cause xGvHD.^{16,21} In this context, von Bonin et al. reported in vivo expansion of cotransplanted T cells within acute myeloid leukemia graft in NSG mice, thereby inducing a severe xGvHD.¹¹

The PDL1 positivity of the WT xenografts described in this report provides a basis for potential benefit of checkpoint inhibitor treatment for patients with lymphocyte-predominant WT. In this context, Holl et al. demonstrated the TIL presence in the tumors of 5 patients with WT and PDL1 expression in one of them. The inflammatory microenvironment of WT with CD3⁺ cell infiltration was previously ascertained in histopathologic evaluation of patients' paraffin-embedded samples.²² Yadav et al. reported numerous TILs in the resected tumors of a series of patients with WT and that higher number of TILs was associated with favorable outcomes.²³ These findings, however, do not factually portend the clinical efficacy of checkpoint inhibitor immunotherapies for WT, and therefore, carefully designed preclinical studies and randomized trials are required in this regard.

For prevention of xGvHD, an unwanted complication in PDX models of solid tumors, potential solutions include but are not limited to:

1. *Use of NSG-β2m^{null} strain for PDX model development:* NSG-β2m^{null} mice are perfect hosts for hematologic and lymphodominant solid tumors, as their MHC class I expression is prevented (due to B2M gene knockout), while additionally have the immunological phenotype of NSG mice. In fact, the risk for xGvHD is minimal when using the NSG-β2m^{null} strain for PDX development.²
2. *Generation of humanized models:* Immunohumanization of young severely immunodeficient mice (such as NOG, NSG, or NRG mice) using human-originated CD34⁺ bone marrow cells or peripheral blood mononuclear cells (PBMCs) can induce a degree of immunologic tolerance in the animal.²⁴ Hence, if an immunodeficient mouse becomes humanized before transplantation of a TIL-dominant tumor xenograft, the resultant immunologic tolerance partially prevents xenogeneic reactions of the cotransplanted TILs.²⁴

3. **Blocking of interleukin 21 (IL-21) signaling:** Hippen et al. showed that administration of neutralizing anti-human IL-21 monoclonal antibody (mAb) to NSG mice (200 µg/mouse, day -1 followed by every 48 h for 6 weeks) can significantly minimize GvHD-associated complications and mortality after xenotransplantation.²⁵
4. **Azacytidine therapy:** Ehx et al. recently demonstrated that 10 injections of 2 or 5 mg/kg of azacytidine (every 48 h from day +1 to day +21) to PBMC-humanized murine models result in increased Tregs and decreased cytotoxic T cells and, consequently, prevention of xGvHD without affecting GvT effects.²⁶
5. **Lymphodepletion of the tumor xenograft:** Although the tumor-infiltrating immune cells are seemingly necessary components for mimicking the tumor microenvironment in PDX model development, lymphocyte depletion of the tumor xenograft via, for example, in vitro incubation with anti-thymocyte globulin (ATG) or anti-CD3 mAbs or corticosteroids before xenotransplantation (during tumor tissue processing), plus short-term injection of these formulations (with serum concentrations equivalent to human doses) to the animals after xenotransplantation might be protective against potential expansion of the TIL posttransplantation and perhaps a solution to prevent xGvHD in PDX models.² Wunderlich et al. showed that the pretreatment of human graft with ATG or anti-CD3 mAbs along with post-xenotransplantation treatment of the PDX models using the same mentioned formulations are able to abolish GvHD risk and preserve engraftment potential of the xenograft.²⁷

5 | CONCLUSIONS

The occurrence of xGvHD after xenotransplantation of high-TIL tumors to severely immunodeficient mice is expectable, as the cotransplanted TILs within the primary xenograft can readily expand inside the host animal. The cotransplanted TILs not only can induce xGvHD, but also may cause lymphoproliferative transformation. Such undesirable disorders can reduce the engraftment rate and animal lifespan, while additionally interfering with the antitumor assays, altering the results, and serving as major confounding factors in anticancer research. Employment of lymphodepletion methods before and after transplantation of the lymphodominant xenografts may salvage the animal host from developing the potential lymphoproliferative transformation and xGvHD.

ETHICS STATEMENT

All experiments were conducted according to institutional standards for the care and use of laboratory animals at Tehran University of Medical Sciences (adopted from AAALAC international guidelines), and reported considering the ARRIVE Guidelines. Protocols involving animal experimentation and human subjects were approved by the Ethics Committee at Tehran University of Medical Sciences (No: IR.TUMS.VCR.REC.1397.169).

AUTHOR CONTRIBUTIONS

Investigation (all authors); validation (Samad Muhammadnejad, Seyed Mostafa Monzavi, Ahad Muhammadnejad); visualization (Samad Muhammadnejad, Seyed Mostafa Monzavi, Ahad Muhammadnejad, Amir Arslan Khorsand); data curation (Samad Muhammadnejad, Seyed Mostafa Monzavi, Ahad Muhammadnejad, Maryam Behfar); formal analysis (Samad Muhammadnejad, Seyed Mostafa Monzavi); writing—original draft (All authors); writing—review and editing (all authors); supervision (Samad Muhammadnejad, Abdol-Mohammad Kajbafzadeh).

ACKNOWLEDGMENTS

Authors would like to acknowledge Cancer Control Foundation, Iran University of Medical Sciences, Tehran, Iran for their kind support (CCF-98049). Authors would also like to thank Ms. Ranjbar and the staff of the PDX Core Laboratory of Digestive Diseases Research Institute, TUMS for their kind cooperation during this study.

FUNDING INFORMATION

This work has been supported by the grant received from Tehran University of Medical Sciences (TUMS-38292)

CONFLICT OF INTEREST

The authors declare no conflicts of interest.

ORCID

Seyed Mostafa Monzavi  <https://orcid.org/0000-0002-1631-1626>

Samad Muhammadnejad  <https://orcid.org/0000-0001-9365-7332>

Abdol-Mohammad Kajbafzadeh  <https://orcid.org/0000-0002-1973-3509>

REFERENCES

1. Ito M, Hiramatsu H, Kobayashi K, et al. NOD/SCID/gamma(c)(null) mouse: an excellent recipient mouse model for engraftment of human cells. *Blood*. 2002;100(9):3175-3182.
2. Muhammadnejad S, Monzavi SM, Khorsand AA, Kajbafzadeh AM. PDX Clinical Trial Design in Anti-Cancer. In: Rahman A, ed. *Topics in Anti-Cancer Research*. Vol 10. Bentham Science Publishers; 2021:100-150.
3. Palmisani F, Kovar H, Kager L, Amann G, Metzelder M, Bergmann M. Systematic review of the immunological landscape of Wilms tumors. *Mol Ther Oncolytics*. 2021;22:454-467.
4. Ullman-Cullere MH, Foltz CJ. Body condition scoring: a rapid and accurate method for assessing health status in mice. *Lab Anim Sci*. 1999;49(3):319-323.
5. Allred DC, Harvey JM, Berardo M, Clark GM. Prognostic and predictive factors in breast cancer by immunohistochemical analysis. *Mod Pathol*. 1998;11(2):155-168.
6. Garon EB, Rizvi NA, Hui R, et al. Pembrolizumab for the treatment of non-small-cell lung cancer. *N Engl J Med*. 2015;372(21):2018-2028.
7. Mohseni MJ, Amanpour S, Muhammadnejad S, et al. Establishment of a patient-derived Wilms' tumor xenograft model: a promising tool for individualized cancer therapy. *J Pediatr Urol*. 2014;10(1):123-129.
8. Jung J, Seol HS, Chang S. The generation and application of patient-derived xenograft model for cancer research. *Cancer Res Treat*. 2018;50(1):1-10.

9. Pompili L, Porru M, Caruso C, Biroccio A, Leonetti C. Patient-derived xenografts: a relevant preclinical model for drug development. *J Exp Clin Cancer Res.* 2016;35(1):189.
10. Williams JA. Using PDX for preclinical cancer drug discovery: the evolving field. *J Clin Med.* 2018;7(3):41.
11. von Bonin M, Wermke M, Cosgun KN, et al. In vivo expansion of co-transplanted T cells impacts on tumor re-initiating activity of human acute myeloid leukemia in NSG mice. *PLoS One.* 2013;8(4):e60680.
12. Ali N, Flutter B, Sanchez Rodriguez R, et al. Xenogeneic graft-versus-host-disease in NOD-scid IL-2R γ null mice display a T-effector memory phenotype. *PLoS One.* 2012;7(8):e44219.
13. Norelli M, Camisa B, Bondanza A. Modeling human graft-versus-host disease in immunocompromised mice. *Methods Mol Biol.* 2016;1393:127-132.
14. Bondarenko G, Ugoikov A, Rohan S, et al. Patient-derived tumor xenografts are susceptible to formation of human lymphocytic tumors. *Neoplasia.* 2015;17(9):735-741.
15. Radaelli E, Hermans E, Omodho L, et al. Spontaneous post-transplant disorders in NOD.Cg-Prkdcscid Il2rgtm1Sug/JicTac (NOG) mice engrafted with patient-derived metastatic melanomas. *PLoS One.* 2015;10(5):e0124974.
16. Tillman H, Vogel P, Rogers T, Akers W, Rehg JE. Spectrum of post-transplant lymphoproliferations in NSG mice and their association with EBV infection after engraftment of pediatric solid tumors. *Vet Pathol.* 2020;57(3):445-456.
17. Fu Q, Chen N, Ge C, et al. Prognostic value of tumor-infiltrating lymphocytes in melanoma: a systematic review and meta-analysis. *Oncoimmunology.* 2019;8(7):1593806.
18. Klein S, Mauch C, Brinker K, et al. Tumor infiltrating lymphocyte clusters are associated with response to immune checkpoint inhibition in BRAF V600(E/K) mutated malignant melanomas. *Sci Rep.* 2021;11(1):1834.
19. Maibach F, Sadozai H, Seyed Jafari SM, Hunger RE, Schenk M. Tumor-infiltrating lymphocytes and their prognostic value in cutaneous melanoma. *Front Immunol.* 2020;11:2105.
20. Valind A, Gisselsson D. Immune checkpoint inhibitors in Wilms' tumor and neuroblastoma: what now? *Cancer Rep (Hoboken).* 2021;4:e1397.
21. Fujii E, Kato A, Chen YJ, Matsubara K, Ohnishi Y, Suzuki M. Characterization of EBV-related lymphoproliferative lesions arising in donor lymphocytes of transplanted human tumor tissues in the NOG mouse. *Exp Anim.* 2014;63(3):289-296.
22. Maturu P, Overwijk WW, Hicks J, Ekmekcioglu S, Grimm EA, Huff V. Characterization of the inflammatory microenvironment and identification of potential therapeutic targets in Wilms tumors. *Transl Oncol.* 2014;7(4):484-492.
23. Yadav DK, Jain V, Dinda AK, Agarwala S. Tumor-infiltrating lymphocytes in Wilms tumor. *Indian J Med Paediatr Oncol.* 2020;41(1):34-38.
24. Morillon YM 2nd, Sabzevari A, Schlom J, Greiner JW. The development of next-generation PBMC humanized mice for preclinical investigation of cancer immunotherapeutic agents. *Anticancer Res.* 2020;40(10):5329-5341.
25. Hippen KL, Bucher C, Schirm DK, et al. Blocking IL-21 signaling ameliorates xenogeneic GVHD induced by human lymphocytes. *Blood.* 2012;119(2):619-628.
26. Ehx G, Fransolet G, de Leval L, et al. Azacytidine prevents experimental xenogeneic graft-versus-host disease without abrogating graft-versus-leukemia effects. *Oncoimmunology.* 2017;6(5):e1314425.
27. Wunderlich M, Brooks RA, Panchal R, Rhyasen GW, Danet-Desnoyers G, Mulloy JC. OKT3 prevents xenogeneic GVHD and allows reliable xenograft initiation from unfractionated human hematopoietic tissues. *Blood.* 2014;123(24):e134-e144.

SUPPORTING INFORMATION

Additional supporting information may be found in the online version of the article at the publisher's website.

How to cite this article: Monzavi SM, Muhammadnejad A, Behfar M, Khorsand AA, Muhammadnejad S, Kajbafzadeh A-M. Spontaneous xenogeneic GvHD in Wilms' tumor Patient-Derived xenograft models and potential solutions. *Anim Models Exp Med.* 2022;5:389-396. doi: [10.1002/ame2.12254](https://doi.org/10.1002/ame2.12254)